Available online at www.synsint.com

Synthesis and Sintering

ISSN 2564-0186 (Print), **ISSN** 2564-0194 (Online)

Research article

Synthesis and characterization of mullite ($3Al_2O_3.2SiO_2$) sol by sol-gel route using inorganic salts

Sahar Sajjadi Milani *, Mahdi Ghassemi Kakroudi, Nasser Pourmohammadi Vafa

Department of Materials Science and Engineering, University of Tabriz, Tabriz, Iran

ABSTRACT

Mullite, also referred to as $3Al_2O_3.2SiO_2$, is recognized as the only chemically stable intermediate phase in the SiO_2–Al_2O_3 system, as indicated by mineralogical studies. Several synthesis techniques can be employed to obtain mullite. In this research, the synthesis of mullite particles is aimed to be achieved via the sol-gel route using inexpensive materials, specifically silica sol and aluminum nitrate hydrate [$(Al(NO_3)_3.9H_2O$] as sources for silica and alumina, respectively. The article is organized into two sections which describe and discuss the systematic synthesis of the mullite sol. The first section emphasizes the influence of the stoichiometric values of Al and Si elements on the formation of the mullite phase at 1200 °C. The effects of sintering temperature on the microstructure and composition of the synthesized mullite sol, with a 3:1 alumina-to-silica ratio, are discussed in the following section. This includes pH, density, solid content, particle size distribution, thermal analysis, phase evolution with temperature, nature of bonds, and microstructural analysis. The XRD results for the mullite sol with a 3:1 alumina-to-silica ratio show strong crystalline diffraction peaks of the mullite phase and the absence of a free silica phase at 1200 °C. The solution exhibits a clear, stable, and homogeneous appearance, with a density of 1.17 g/cm^3, a pH ranging from 4 to 5, and a solid content of approximately 15%, measured after heating at 1000 °C for 2 h.

KEYWORDS

Mullite
Sol-gel
Inorganic route
Chemical synthesis

OPEN ACCESS

1. Introduction

Mullite is a ceramic material composed of aluminosilicate ($3Al_2O_3.2SiO_2$) that is widely used due to its exceptional chemical and physical properties. It is recognized for its excellent mechanical strength, high melting point, resistance to abrasion and oxidation, and durability against corrosive furnace atmospheres. Additionally, mullite exhibits excellent creep resistance at high temperatures, good chemical stability, low thermal expansion (4.5×10^{-6} °C^{-1}), a low dielectric constant, and low thermal conductivity (6×10^{-2} W.cm^{-1}.K^{-1}) [1,2]. Due to these unique properties, mullite finds diverse usages across structural, coating, chemical, optical, and electrical fields. Its applications include serving as an optical component in infrared windows, a binder in refractory castables, kiln setting slabs and posts for firing ceramics, a catalyst carrier, and a gas-permeable ceramic element [3–5].

The synthesis technique and the choice of raw components play crucial roles in influencing the palletization temperature, reaction mechanisms, and product homogeneity during the formation of mullite. Since mullite is rarely found in nature, it is typically synthesized rather than extracted through mining. The synthesis of mullite can be classified into various methods based on the starting materials and routes employed [6, 7]:

- Solid-state-derived mullite.
- Liquid-state-derived mullite
- Vapor-state-derived mullite
- Solution-sol-gel-derived mullite
- Spray pyrolysis
- Hydrothermally

* Corresponding author. *E-mail address:* sahar.sajjadi@tabrizu.ac.ir (S. Sajjadi Milani)
Received 20 July 2024; Received in revised form 24 December 2024; Accepted 24 December 2024.

https://doi.org/10.53063/synsint.2024.44235

The characteristics of mullite such as purity, homogeneity, crystallization temperature, and compaction are influenced by the synthesis method. Each method possesses distinct characteristics that are determined by the application and purity of the mullite produced. The sol-gel technique is commonly used for synthesizing mullite due to its cost-effectiveness, simple setup, high specific surface area, high purity, homogeneity, ability to form at relatively lower temperatures, and good reproducibility. Various parameters, including water content, raw materials, pH, and inorganic and organic additives, influence the rates of hydrolysis and condensation reactions in sol-gel methods [8, 9].

For example, previous studies have shown that higher pH levels lead to an increase in particle size, while acidic conditions favor the generation of smaller particles. Different sources of alumina and silica have been used for the formation of mullite sol ($3Al_2O_3.2SiO_2$). Several inorganic salts (e.g., chloride, acetate, sulfate, and nitrate) or organic compounds (metal alkoxides) are used as precursors. Tan et al. [10] synthesized mullite fibers using the sol-gel method with silica and alumina as starting materials. They found that the complete nullification occurred at 1000 °C. The calcined fibers had uniform diameters and smooth surfaces. The mullite homogeneity and synthesis conditions via the sol-gel method resulted in various types of gels that could be categorized into three types:

- Monophasic gel: if the mixing of Si and Al atoms happens at the atomic level.
- Diphasic gel: if the level of homogeneity is between 1 and 100 nm.
- Hybrid gel: if an integration of monophasic and diphasic takes place.

Monophasic gels may be achieved through slow alkoxides hydrolysis and salt solution mixtures. The synthesis and analysis of sol-gel-derived mullite monophasic powders were studied by Jana et al. [11]. They synthesized mullite powder using an aqueous solution of tetraethyl orthosilicate (TEOS) and aluminum isopropoxide (AIP). Their research discloses that the synthesized mullite has homogeneity in the blending scale of the aluminum-silicon components, resulting in an exothermic peak. The formation of tetragonal mullite at 980 °C is verified by XRD testing. Wang et al. [12] successfully synthesized diphasic mullite gels using the sol-gel process from boehmite sol and silica sol, employing varying concentrations of alumina and silica. The study demonstrated that the structural evolution, mullite formation temperature, and densification behavior are significantly influenced by the homogeneity of the gels. Gels with higher homogeneity exhibited mullite crystallization at lower temperatures, which leads to poorer densification behavior due to overlap with the temperature range required for densification through viscous flow and reactive sintering. The initial generation of silica-alumina spinel at approximately 950 °C was facilitated by the inclusion of ammonium nitrate in the gels, which then reacts with free SiO_2 to produce elongated grains of orthorhombic mullite at around 1250 °C. Consequently, sol-gel technology plays a critical role in various aspects of materials science, including the nuclear, ceramics, refractory, and electronics industries. Notably, the use of ceramic sols (such as alumina, spinel, mullite, silica, etc.) has introduced new bonding systems in the refractory industries [13, 14]. The gel formation from a sol that encircles the refractory particles serves as the basis for the bonding system. Upon heating, the gel bonding system is replaced by a ceramic bonding system. The sintering of these ceramic bonds at the interfaces of refractory particles enhances the strength of the refractory body. Research by Singh et al. [15] on the synthesis of mullite sol was carried out using a wet chemical synthesis route. This sol was utilized as a binder in pure Al_2O_3 refractories with two different particle size distributions. It was found that a basic tapping method could be economical. Heat treatment of the sol before use activated it, increasing the solid content and enhancing the physical characteristics of the castables. In another study, Mukhopadhyay et al. [16] synthesized mullite and spinel sols using a cheaper precursor of Al_2O_3 sol. The effects of spinel and mullite sols as binders in ultra-low cement high-alumina-based castables were examined. The study concluded that mullite sol outperforms spinel sol due to its homogeneity and high reactivity with micro-fine particles, whereas spinel sol negatively impacts the quality of refractory castables.

The present study aims to synthesize mullite ($3Al_2O_3.2SiO_2$) nanoparticles via a simple cost-effective route. The colloidal suspensions of mullite are derived from silica sol and aluminum nitrate hydrate [$Al(NO_3)_3.9H_2O$]. The synthesized sol will be characterized for various properties, including solid content, pH, phase composition, particle size, thermal behavior, and microstructure at different temperatures.

2. Experimental

2.1. Materials and processes

In the present paper, the nanostructured mullite particles are synthesized by a sol-gel process through an inorganic route. The used starting materials in the formation of mullite sol were aluminum nitrate nonahydrate ($Al(NO_3)_3.9H_2O$) (purity >98%, Merck, Germany) as an alumina source, silica sol (25% SiO_2, CAS No.: 7631-86-9, Iran) as a silica source, ammonia (25%, Merck, D-6100 Darmstadt, Germany), nitric acid (E. Merck, purity > 99%, F.R. Germany), and deionized water (1 $g.cm^{-3}$, Dr. Mojallali Industrial Chemical, Iran). For mullite sol preparation, aluminum nitrate solution was dissolved in silica sol at varying ratios (alumina-to-silica of 2:4, 2:3, 3:2, and 3:1, identified as M4, M3, M2, and M1, respectively) with vigorous stirring using a magnetic stirrer (d500, Alfa, Iran) for 1 hour at 25 °C. Then, ammonia solution, in a stoichiometric amount relative to the alumina source, was gradually added under vigorous stirring for 5 hours to prevent precipitation. Adding ammonia enhances the pH and viscosity of the colloidal suspension [17]. Finally, a stable clear mullite precursor sol was achieved. The method for preparing the mullite sol is detailed in Fig. 1. The mullite sol forms a gelled network when heated above 60 °C in a rotary evaporator (Tebazma HMS 14, Iran). The gel was then converted into mullite nanoparticles by further heating at 1000 °C in an oven (Azar Furnace Co., M11L-1100, Iran).

2.2. Characterization

Various analyses were conducted to investigate the microstructure and characterization of the synthesized sol. The solid content was assessed using the loss on ignition technique after firing at a temperature of 1000 °C for 2 h, while pH was measured with a digital pH meter (AZ, model 8686). Particle size distribution was measured using dynamic light scattering (DLS: Nanotrac Wave model, Microtrac Co.), while density was evaluated through a pycnometer. The presence of bonds was analyzed via Fourier transform infrared spectroscopy (FTIR: Bruker Co., Germany), and thermal characteristics were evaluated using thermal gravimetric analysis and differential scanning calorimetry (DSC-TG: TA-Q600, USA). Phase analysis was performed

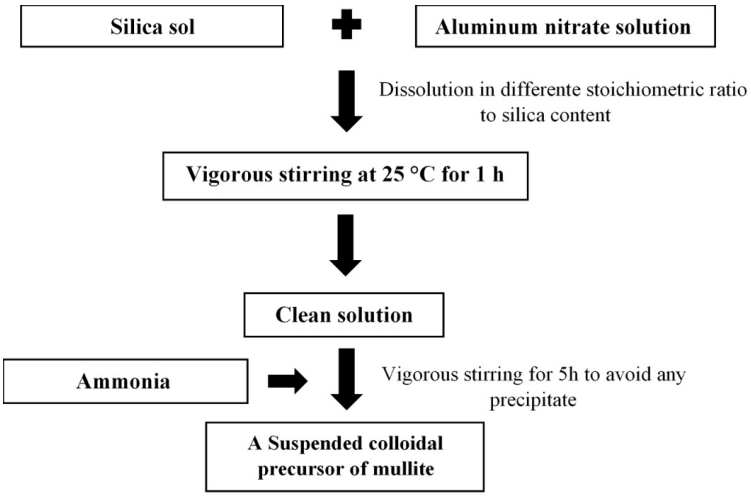

Fig. 1. Flowchart of mullite sol synthesis via inorganic route.

through X-ray diffraction, employing, a step time of 0.3 s, a step size of 0.02, Cu Kα at 30 mA and 40 kV within the 2θ range of 20 °–80° at a scanning speed of 5 °/min (D5000, Siemens, Germany). Additionally, the morphology and microstructure studies of the dried and calcined sol particles were conducted using field emission scanning electron microscopy (FESEM: Tescan Mira 3, Czech Republic), complemented by energy dispersive spectroscopy (EDS: digital X-ray DXP-X10P processor) for elemental evaluation.

3. Results and discussion

In this section, the results and phase analysis of mullite sol using the XRD method will be discussed. Fig. 2 presents the XRD spectra of powders synthesized at 1200 °C from mullite sols with different alumina-to-silica ratios (M1=3:1, M2=3:2, M3=2:3, and M4=2:4). It was observed that M4 exhibits weak crystalline diffraction peaks corresponding to the mullite phase and free silica phase at 1200 °C. Comparing the XRD patterns of mullite sols with varying alumina and silica contents reveals that, in M1, the intensity of all orthorhombic mullite phase peaks significantly increased, with no free silica detected at 1200 °C. This confirms that factors such as particle size, Al_2O_3/SiO_2 ratio, purity, and degree of mixing influence the chemical reaction involved in mullite formation.

Here, the properties and characteristics of mullite sol M1 prepared via the chemical route are investigated by solid content, density measurement, thermal analysis, particle size distribution, phase formation as a function of temperature, microstructural, and FTIR analysis. The stability of the synthesized mullite sol M1 is presented in Fig. 3, showing transparency and stability for over 2 months at 25 °C (room temperature). The mullite sol possesses a density of 1.17 g/cm^3 and a pH value of 5. When the temperature exceeds 40 °C, the sol turned into a gel due to water loss over time. The average solid content of the sol, determined through the loss on ignition technique at 1000 °C for 2 h, is approximately 15%. As can be seen in Fig. 4, dynamic light scattering (DLS) in dilute conditions reveals that all particles of mullite sol fall within the 10–1000 nm size range. This particle size in nanometers enables the particles to exhibit Brownian motion, preventing sedimentation, and maintaining sol stability for over 2 months.

The characteristic bands in the mullite sol were examined using Fourier transform infrared spectroscopic (FTIR) analysis. The FTIR results of mullite powder dried at 200 °C in the wavenumber region 500–1400 cm^{-1} are depicted in Fig. 5. The mullite band appeared at around 550, 720, 850, and 1170 cm^{-1} in the spectra. The peaks at 550

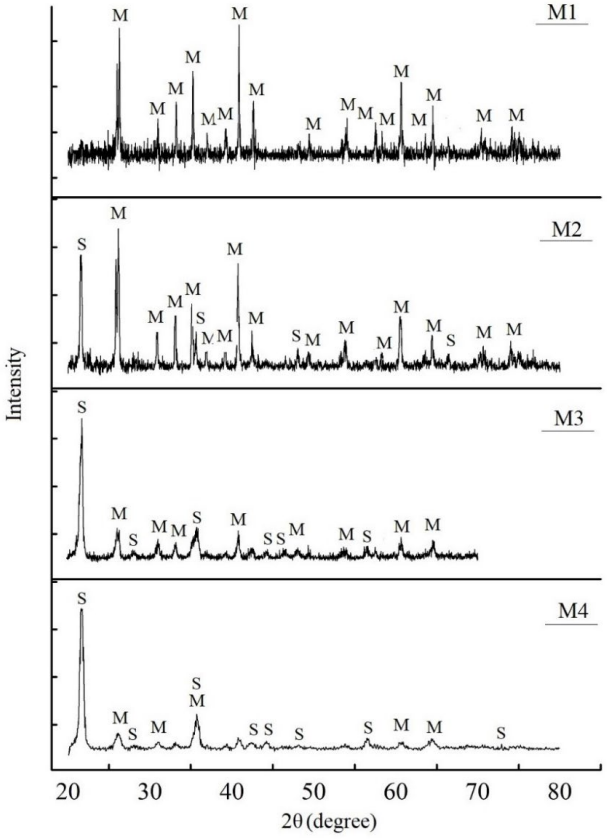

Fig. 2. The X-ray diffraction patterns of mullite sol with various ratios of alumina-to-silica content heated at 1200 °C (M: mullite and S: silica).

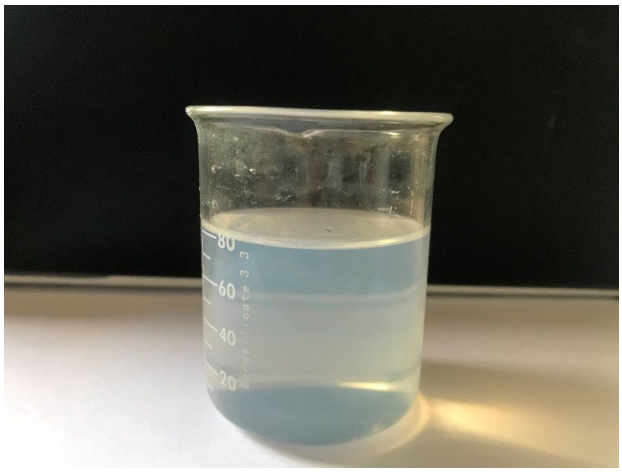

Fig. 3. Stable mullite sol (M1) prepared from inorganic precursors.

and 850 cm^{-1} correspond to the stretching vibration of Al–O in alumina octahedral and tetrahedral (AlO_6 and AlO_4), respectively. The peak at 720 cm^{-1} might be attributed to the bending vibrations of Al–OH. It seems that the presence of a band at about 1170 cm^{-1} is due to the stretching vibration of Si–O in silica tetrahedral (SiO_4) [18]. Additionally, bands appearing at approximately 1385 cm^{-1} are attributed to the stretching vibration of the residual nitrates (NO_3) group [19–21]. Based on the above analysis, the broad bands observed in the range of 1640 and 3200 cm^{-1} in the spectrum correspond to the –OH stretching vibration and the deformation vibrations of H–O–H, respectively. These bands are attributed to the presence of structural molecular water. No vibration related to metal-oxide-metal bonds is observed due to the lack of Si–O–Al (mullite) bond formation at 200 °C.

The mechanism of the formation of mullite nanoparticles is followed by thermal analysis. The simultaneous differential scanning calorimetry and thermogravimetric (DSC-TG) curves of the powder derived from mullite sol (M1) after drying at 200 °C were presented in Fig. 6. Although dried at 200 °C, the powder obtained from mullite sol has absorbed some environmental moisture due to its hygroscopic nature. In the DSC pattern, a broad endothermic peak between 60–200 °C is observed, likely due to the evaporation of physically bonded absorbed water, which is supported by the weight loss observed in the TG diagram at the same temperature. The next outstanding and sharp endothermic peaks at around 280 and 500 °C can be attributed to the conversion of aluminum trihydrate ($Al(OH)_3$) to boehmite (AlO(OH)) and slow dehydration of boehmite to γ-Al_2O_3, as illustrated in Eq. 1 & 2, respectively.

$$Al(OH)_3 \rightarrow AlO(OH) + H_2O \quad (1)$$

$$2AlO(OH) \rightarrow Al_2O_3 + H_2O \quad (2)$$

According to the previous study, the exothermic reaction around 350 °C is associated with the decomposition of ammonium nitrate (NH_4NO_3) [14]. Some of the ammonium nitrate decomposition reactions mentioned in the sources are as follows [20]:

$$NH_4NO_3 \rightarrow N_2 + 2H_2O + \frac{1}{2}O_2 \quad (3)$$

$$NH_4NO_3 \rightarrow N_2O + 2H_2O \quad (4)$$

$$NH_4NO_3 \rightarrow \frac{1}{2}N_2 + 2H_2O + NO \quad (5)$$

$$NH_4NO_3 \rightarrow N_2 + H_2O + \frac{1}{2}O_2 \quad (6)$$

A tiny and broad endothermic peak around 950 °C is observed during the further heating of mullite powder, which is likely attributed to the phase transformation of γ-Al_2O_3 to α-Al_2O_3. The crystallization of mullite (nullification), formed from a well-mixed blend of the α-Al_2O_3 phase and amorphous silica, is indicated by the final broad endothermic peak in the DSC diagram at approximately 1150 °C. This is supported by X-ray diffraction analysis (Fig. 2), which shows the formation of mullite with no evidence of free silica at 1200 °C. The TG plot (Fig. 6) shows weight loss occurring between 200 and 400 °C, accounting for approximately 80% of the total weight loss. This can be attributed to the elimination of bonded (OH) groups and decomposition reactions, including the decomposition of ammonium nitrate at 350 °C. After 600 °C, almost no weight loss is observed in the TG plot, which was due to the onset of crystallization.

The field emission scanning electron microscopy was employed to assess the impact of sintering on microstructural evolution. The FESEM images along with EDS results of the mullite, sol dried at 200 °C and sintered at 1200 °C are illustrated in Figs. 7 & 8.

The micrographs (Fig. 7) reveal highly agglomerated particles on the

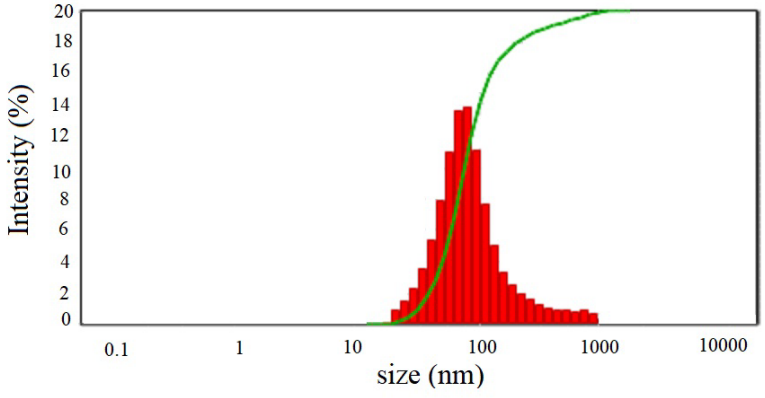

Fig. 4. Diagram of the particle size distribution for the synthesized mullite sol (M1).

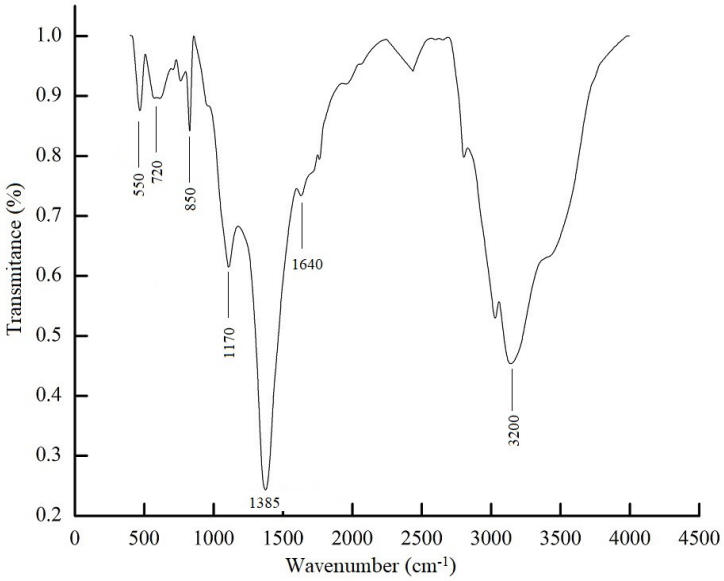

Fig. 5. The Fourier transform infrared (FTIR) spectroscopy of dried mullite sol (M1) at 200 °C.

surface at lower temperatures, along with smaller distributed and agglomerated particles of varying shapes and sizes. These aggregated particles may result from the reaction of raw materials, as well as the high surface area and intense reactivity of the sol particles, as indicated by the formation of various phases. As it is shown in Fig. 7, the average diameter of the mullite sol at 200 °C is below 40 nm. After heat treatment at 1200 °C and conversion to mullite particles, the mean grain sizes, measured around 35–50 nm as shown in Fig. 8, are observed due to grain growth during the 120-minute calcination period. The EDS results of the particles dried at 200 °C show no significant difference compared to those sintered at 1200 °C. Peaks for Al, O, Si, and N are observed in both specimens, with the N peak attributed to residual nitrate. At 1200 °C, the intensity of the N and O peaks weakened compared to 200 °C, due to the reduction of residual nitrides (Eqs. 3, 4, 5, and 6) and the removal of absorbed water (Eqs. 1 and 2), respectively. Additionally, the intensity of the Al and Si peaks is intensified at 1200 °C, indicating the formation of mullite particles. This study aimed to produce mullite sol using cost-effective precursors, including aluminum nitrate salt, silica sol, and ammonia, via the sol-gel method. Previous studies have successfully synthesized alumina [13] and spinel [14] sols using the inorganic sol-gel process. The impact of incorporating synthesized alumina, spinel, and mullite sols into alumina spinel as a substitute for cement will be explored in a separate investigation.

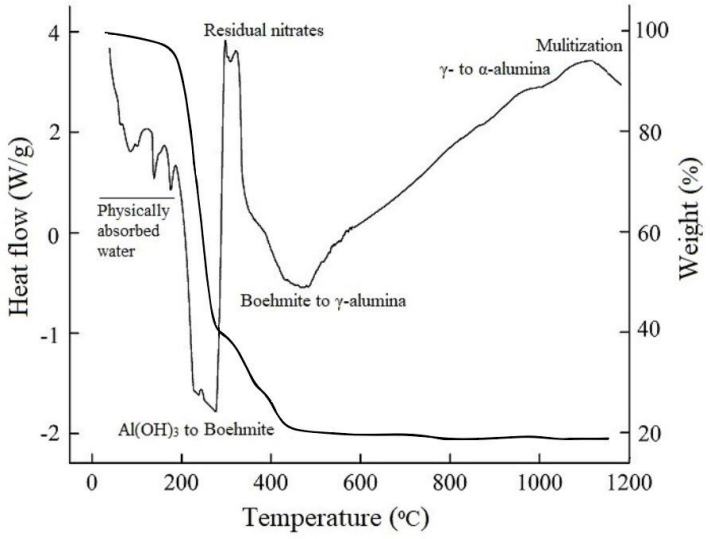

Fig. 6. The DSC-TG results of mullite precursor sol (M1) dried at 200 °C.

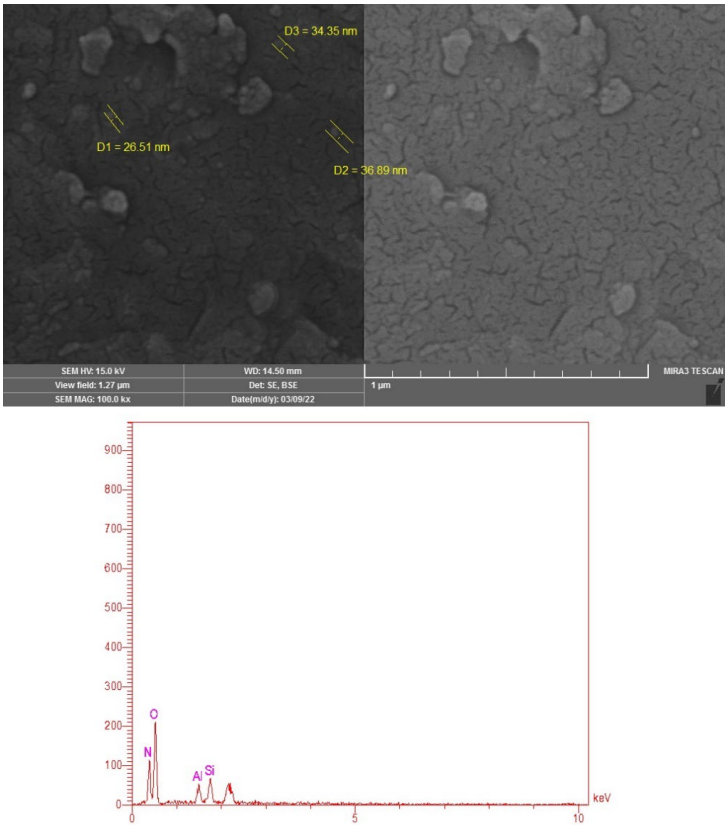

Fig. 7. FESEM image and EDS of mullite sol (M1) dried at 200 °C.

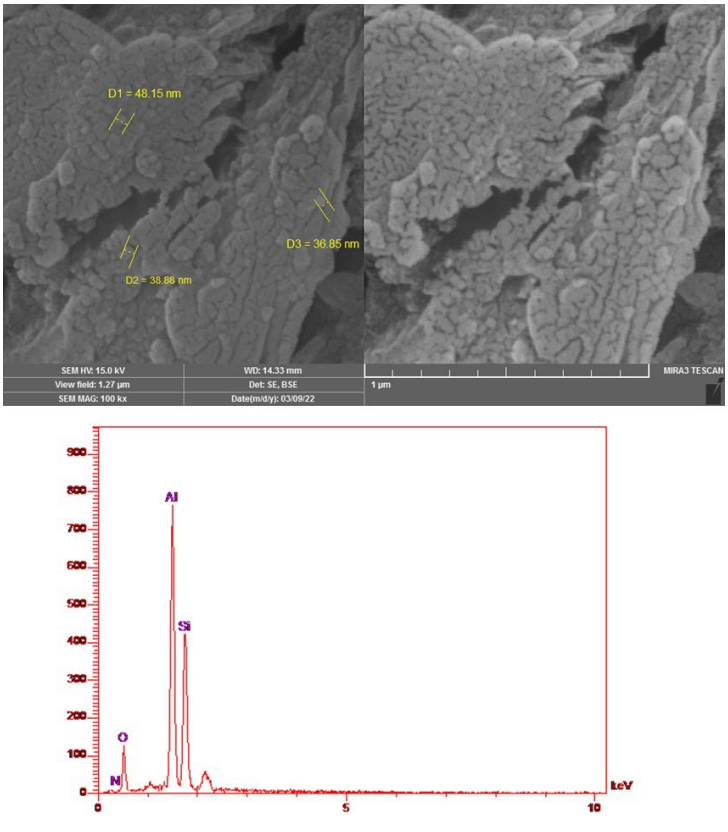

Fig. 8. FESEM image and EDS of mullite sol (M1) sintered at 1200 °C.

4. Conclusions

In this research, the mullite particles were synthesized via a wet chemical route (sol-gel technique) employing inexpensive materials, including silica sol and aluminum nitrate hydrate [$(Al(NO_3)_3.9H_2O$] as the source for silica and alumina, respectively. The particles were analyzed for solid level, pH, particle size, density, FTIR, DSC-TG, phase analysis, and microstructure evaluation at various calcination temperatures. The formation of post-calcination pure nano-oxides is indicated by different methods for characterizing sols. Mullite formation from the synthesized mullite sol, which contained a 3:1 ratio of alumina-to-silica, could be achieved by calcination at around 1200 °C. The resulting mullite sol has a solid content of ~15%. The FTIR and DSC-TG analysis on the mullite powder dried achieved from the sol verifies the presence of mullite. Based on the FESEM micrographs, the grain size of the sample calcined at 1000 °C for 2 h is estimated to range from 30 to 50 nanometers.

CRediT authorship contribution statement

Sahar Sajjadi Milani: Writing – original draft, Visualization, Investigation.
Mahdi Ghassemi Kakroudi: Writing – review & editing, Project administration.
Nasser Pourmohammadi Vafa: Writing – review & editing.

Data availability

The data underlying this article will be shared on reasonable request to the corresponding author.

Declaration of competing interest

The authors declare no competing interests.

Funding and acknowledgment

The authors would like to acknowledge the Advanced Ceramic Research Group (ACRG) of the University of Tabriz, Iran for its helpful support.

References

[1] L.S. Cividanes, T.M.B. Campos, L.A. Rodrigues, D.D. Brunelli, G.P. Thim, Review of mullite synthesis routes by sol–gel method, J. Sol-Gel Sci. Technol. 55 (2010) 111–125. https://doi.org/10.1007/s10971-010-2222-9.

[2] S. Sembiring, W. Simanjuntak, P. Manurung, D. Asmi, I.M. Low, Synthesis and characterisation of gel-derived mullite precursors from rice husk silica, Ceram. Int. 40 (2014) 7067–7072. https://doi.org/10.1016/j.ceramint.2013.12.038.

[3] P. Pialy, N. Tessier-Doyen, D. Njopwouo, J.P. Bonnet, Effects of densification and mullitization on the evolution of the elastic properties of a clay-based material during firing, J. Eur. Ceram. Soc. 29 (2009) 1579–1586. https://doi.org/10.1016/j.jeurceramsoc.2008.09.020.

[4] A. Abdullayev, D. Klimm, F. Kamutzki, A. Gurlo, M.F. Bekheet, AlF3-assisted flux growth of mullite whiskers and their application in fabrication of porous mullite-alumina monoliths, Open Ceram. 7 (2021) 100145. https://doi.org/10.1016/j.oceram.2021.100145.

[5] D. Das, N. Kayal, G.A. Marsola, D.G.Parra. Filho, M.D.M. Innocentini, Recycling of coal fly ash for fabrication of elongated mullite rod bonded porous SiC ceramic membrane and its application in filtration, J. Eur. Ceram. Soc. 40 (2020) 2163–2172. https://doi.org/10.1016/j.jeurceramsoc.2020.01.034.

[6] R. Baranwal, M.P. Villar, R. Garcia, R.M. Laine, Flame Spray Pyrolysis of Precursors as a Route to Nano-mullite Powder: Powder Characterization and Sintering Behavior, J. Am. Ceram. Soc. 54 (2001) 951–961. https://doi.org/10.1111/j.1151-2916.2001.tb00774.x.

[7] X. Song, Y. Ma, J. Wang, B. Liu, S. Yao, et al., Homogeneous and flexible mullite nanofibers fabricated by electrospinning through diphasic mullite sol–gel route, J. Mater. Sci. 53 (2018) 14871–14883. https://doi.org/10.1007/s10853-018-2667-8.

[8] N.M. Khalil, M.B. Hassan, E.M.M. Ewais, F.A. Saleh, Sintering, mechanical and refractory properties of MA spinel prepared via co-precipitation and sol–gel techniques, J. Alloys Compd. 496 (2010) 600–607. https://doi.org/10.1016/j.jallcom.2010.02.123.

[9] L.T. Jurado, R.M.A. Hernandec E. Rocha-Rangel, Sol-Gel Synthesis of Mullite Starting from Different Inorganic Precursors, J. Powder Technol. 2013 (2013) 268070. https://doi.org/10.1155/2013/268070.

[10] H. Tan, Y. Ding, J. Yang, Mullite fibers prepared from an inorganic sol–gel precursor, J. Sol–Gel Sci. Technol. 53 (2010) 378–38. https://doi.org/10.1007/s10971-009-2106-z.

[11] A. Jana, D. Ray, Synthesis and characterization of sol-gel derived monophasic mullite powder, Cerâmics. 66 (2020) 307–313. https://doi.org/10.1590/0366-69132020663792907.

[12] Y. Wang, H. Liu, H. Cheng, J. Wang , Densification behavior and microstructure of mullite obtained from diphasic, Ceram. Int. 40 (2014) 12789–12796. https://doi.org/10.1016/j.ceramint.2014.04.133.

[13] S.S. Milani, M.G. Kakroudi, N.P. Vafa, M.M. Mokhayer, S.H. Gharamaleki, Properties of alumina sol prepared via inorganic route, Ceram. Int. 46 (2020) 9492–9497. https://doi.org/10.1016/j.ceramint.2019.12.210.

[14] S.S. Milani, M.G. Kakroudi, N.P. Vafa, S. Rahro, F. Behboudi, Synthesis and characterization of MgAl2O4 spinel precursor sol prepared by inorganic salts, Ceram. Int. 47 (2021) 4813–4819. https://doi.org/10.1016/j.ceramint.2020.10.051.

[15] A.K. Singh, R. Sarkar, Nano mullite bonded refractory castable composition for high temperature applications, Ceram. Int. 42 (2016) 12937–12945. https://doi.org/10.1016/j.ceramint.2016.05.066.

[16] S. Mukhopadhyay, S. Ghosh, M.K. Mahapatra, R. Mazumder, P. Barick,et al., Easy-to-use mullite and spinel sols as bonding agents in a high-alumina based ultra low cement castable, Ceram. Int. 28 (2002) 719–729. https://doi.org/10.1016/S0272-8842(02)00034-2.

[17] A.K. Singh, R. Sarkar, Development of spinel sol bonded high pure alumina castable composition, Ceram. Int. 42 (2016) 17410–17419. https://doi.org/10.1016/j.ceramint.2016.08.041.

[18] P. Sultana, S. Das, B. Bagchi, A. Bhattacharya, R. Basu, P. Nandy, Effect of size of fly ash particle on enhancement of mullite content and glass formation, Indian Acad. Sci. 34 (2011) 1663–1670. https://doi.org/10.1007/s12034-011-0374-z.

[19] A. Saberi, F.Golestanifard, H. Sarpoolaky, M. Willert-porado, T. Gerdes, R. Simon, Chemical synthesis of nanocrystalline magnesium aluminate spinel via nitrate-citrate combustion route, J. Alloy Compd. 462 (2008) 142–146. https://doi.org/10.1016/j.jallcom.2007.07.101.

[20] S.Biamino, C.Badini, Combustion synthesis of lanthanum chromite starting from water solutions: Investigation of process mechanism by DTA–TGA–MS, J. Eur. Ceram. Soc. 24 (2004) 3021–3034. https://doi.org/10.1016/j.jeurceramsoc.2003.10.005.

[21] S.S. Milani, M.G. Kakroudi, M. Rezvani, The effects of processing technique on formation temperature of calcium aluminate magnesium (CaO.2MgO.8Al2O3), Cryst. Growth. 643 (2024) 17797. https://doi.org/10.1016/j.jcrysgro.2024.127797.